



Deposited via The University of Leeds.

White Rose Research Online URL for this paper:

<https://eprints.whiterose.ac.uk/id/eprint/111092/>

Version: Accepted Version

Article:

Aliyu, MM, Murphy, W, Lawrence, JA et al. (2017) Engineering geological characterization of flints. *Quarterly Journal of Engineering Geology and Hydrogeology*, 50 (2). pp. 133-147. ISSN: 1470-9236

<https://doi.org/10.1144/qjegh2015-044>

© 2017 The Author(s). Published by The Geological Society of London. This is an author produced version of a paper published in *Quarterly Journal of Engineering Geology and Hydrogeology*. Uploaded in accordance with the publisher's self-archiving policy.

Reuse

Items deposited in White Rose Research Online are protected by copyright, with all rights reserved unless indicated otherwise. They may be downloaded and/or printed for private study, or other acts as permitted by national copyright laws. The publisher or other rights holders may allow further reproduction and re-use of the full text version. This is indicated by the licence information on the White Rose Research Online record for the item.

Takedown

If you consider content in White Rose Research Online to be in breach of UK law, please notify us by emailing eprints@whiterose.ac.uk including the URL of the record and the reason for the withdrawal request.

1

2 **Engineering Geological Characterisation of Flints**

3 Mohammed Musa Aliyu¹, William Murphy¹, James Anthony Lawrence² and Richard Collier¹

4 ¹Institute of Applied Geosciences, School of Earth and Environment, University of Leeds,
5 Leeds, LS2 9JT (UK)

6 ²Department of Civil and Environmental Engineering, Imperial College London, Skempton
7 Building, London, SW7 2AZ

8 **Abstract**

9 The petrographic and mechanical properties of flints from the Burnham (North Landing,
10 Yorkshire, UK), Seaford (East Sussex, UK, and Dieppe, France), and Lewes Nodular (Mesnil-
11 Val-Plage, France) Chalk Formations have been investigated. Microtexture and mineral
12 composition of flints are studied to understand how the geological and petrophysical properties
13 of the flint affect drilling responses to the rock and investigate any spatial variation. The flints
14 are categorised based on physical observation: white crust; light brown; brown grey, dark-
15 brownish-grey and grey flints. Scanning electron microscopy shows textural variation in the
16 classes. The white crust surrounding the light brownish grey, brownish grey and grey flints
17 from Burnham Chalk Formation, from North Landing, in Yorkshire contain more calcite and
18 have coarser more poorly cemented silica spherules by comparison to similar classes of flint
19 from the Seaford and Lewes Chalk Formations from the Anglo-Paris Basin. In these latter
20 flints, the structure is dominated by massive quartz cement with trace calcite independent of
21 location. Strength tests show that the grey flints from North Landing are weaker than
22 equivalents from the Anglo-Paris Basin. It is suggested that variation in engineering properties
23 between grey and the dark brownish grey flints is caused by mineral composition, microtexture,
24 structure and the local/site geology of flint materials.

25

26

27 *Keywords:* Engineering; Flint; Chalk; mechanical; properties; Mineralogy; Microstructure

28 **Introduction**

29 Flint is a siliceous, cryptocrystalline rock that forms in chalk. They are primarily composed
30 of silica (87%-99%) with small amounts of calcite and clay minerals. It exists within chalk
31 units and is found widely in Europe, parts of the USA and the Middle East. Flint has various
32 morphologies (Fig.1): sheet; tabular; tubular; nodular; and Paramoudra (barrel shaped)
33 (Bromley 1967; Clayton 1984; 1986).

34 The distribution of chalk in the Thames and Paris Basin means that it is often intercepted
35 during drilling and engineering projects. Drilling is carried out for resource exploitation
36 including e.g. water resources for instance in the UK, Denmark, Jordan and Israel and for
37 hydrocarbons, for instance in the North Sea Basin (Mortimore, 2012) and also during ground
38 investigations. Engineering projects include tunnelling for infrastructure such as for High
39 Speed 1 (formally The Channel Tunnel Rail Link) Crossrail 1 and the Lee Tunnel Project both
40 in south east England. Drilling and construction in the chalk can be affected by flints as they
41 are generally extremely strong which contrasts with the very weak to weak chalk. These are
42 also hard due to their silica content, resulting in significant wear and reduced rates of
43 penetration (ROP) of drilling bits and the cutting heads of tunnel boring machines (TBM). As
44 such they present a significant construction risk and should be incorporated into risk registers
45 associated with the geotechnical baseline reports and the geological models. As a results this
46 work provides a detailed investigation of what effects flints mechanical properties and
47 behaviour within the context of their geological setting and the impact this may have on
48 geotechnical projects in the chalk.

49 **Background**

50 The mineralogical and chemical compositions of flints have received considerable attention
51 in both archaeology and the geosciences. In archaeology, various geochemical techniques have
52 been employed for provenance studies to constrain the origins of flint artefacts (e.g. Olausson
53 *et al.* 2012; Huges *et al.* 2012; Prudêncio *et al.* 2015). For the most part these studies, which are
54 only examples of a wider field, draw on the colour and geochemistry of flints to identify their
55 provenance.

56 In addition to the identification of sources, the use of flints as tools by early mankind has
57 been investigated. Pradel & Tourenq (1967) investigated the strength and hardness of Grand-
58 Pressigny Flint with a comparison to other potential tool materials (coarse sandstone and
59 Jasper-Opal) and noted that the Grand-Pressigny Flint was the most durable rock among the

60 Palaeolithic geo-materials investigated. Domański & Webb (2000) correlated the grain size,
61 mineralogy and the microfracturing and compared these parameters to the measured fracture
62 toughness to characterise their flaking properties and found that these parameters exerted a
63 clear control on the ability of flints to maintain a good cutting edge.

64 In the geosciences, X-Ray diffraction (XRD) has been used to investigate the mineralogy
65 of flint using qualitative and quantitative approaches (e.g. Graetsch & Grunberg 2012;
66 Jakobsen *et al.* 2014). Energy Dispersive X-ray Spectroscopy (EDX) (Wasilewski 2002) and
67 Energy Dispersive X-ray Fluorescence (EDXRF) analysis (Hughes *et al.* 2010) has also been
68 applied to investigate the mineralogy of flints. It was established that α -quartz is the major
69 mineral phase in flint with minor amounts of calcite and clay minerals.

70

71 ***Mineralogy and geological observations***

72 Jeans (1978) recognised that the mineral composition of flint is non-uniform noting a
73 differentiation between the flint core and the cortex (the original outer layers). The presence of
74 different quartz phases in various flint samples was also noted. Clayton (1984) carried out
75 detailed microstructural studies on flints and associated crusts and provides an explanation of
76 textural compositions and growth sequence of flints and the surrounding crust. Madsen &
77 Stemmerik (2010) differentiated between white and dark flints and showed that the dark flint
78 possessed more massive silica cements than the white flint. Although variations in micro-
79 structural/textural details combined with colour and structures of flints were investigated, the
80 relationship between micro-structure/textures and the mechanical properties (especially the
81 strength) of various flint morphologies (Fig. 1) from different regions remains unresolved.

82

83 ***The mechanical properties of flints***

84 The variability of micro-structures/texture, chemical and mineral compositions of flint is
85 reflected in the mechanical characteristics of flint. Iller (1963) examined the transverse rupture
86 strength of flints and concluded that the fine grain nature of flints contributes to their strength.
87 Since this work, a variety of different measures of the mechanical properties of flint have been
88 investigated. These include Uniaxial Compressive Strength (UCS) (Varley 1990), tensile
89 strength (Cumming 1999) and point load strength (Smith *et al.* 2003) with studies normally
90 involving more than one test. While flints are generally considered to be extremely strong,
91 considerable variability is observed. Cumming (1999) noted that weathered, fractured, carious
92 (flint with network of crumbly, poorly silicified chalk) and pale flints from the White Chalk
93 Subgroup of the Southern Province, UK, had lower strengths by comparison to other flints.

94 Such variability was attributed to the presence of internal microfractures associated with the
95 flint samples. These observations were supported by the work of Smith *et al.* (2003) who
96 suggested that the variation in material/strength properties of flints might also depend on its
97 geographical location which is suggestive of mineralogical or macrostructural controls.

98 In this paper the mineralogy and mechanical properties of flints of different morphologies
99 from three regions are described. The description is in terms of the mineralogy, strength,
100 elasticity and abrasivity. The relationships between flint strength, deformation properties,
101 morphology, microtexture and colour are described with the aim of providing useful guidance
102 for engineers and geoscientists at the desk study stage of a ground investigation. A
103 classification of flints based on colour is proposed.

104 **Materials and Methods**

105 *Descriptions of flint*

106 The nomenclature for samples is as follows: the first letter relates to the formation; the
107 second/third relates to geographic location; and the final fourth or fifth letter relates to the
108 country. For example, flints sampled from the Burnham Chalk Formation at North Landing in
109 the UK are given the notation B-NL-UK (BNLUK).

110 The test materials were from the Burnham Chalk Formation, North Landing, Yorkshire,
111 UK (BNLUK) [TA 243 706], the Seaford Chalk Formation, East Sussex, UK (SESUK) [TA
112 675 510] and at Dieppe, France (SDFr) [TW 196 769], and the Lewes Chalk Formation at
113 Mesnil-Val-Plage, France (LMFr) [TW 539 265] (see Fig. 2). Samples were collected from
114 sea-cliff exposures and occasionally, from fresh rock falls where the stratigraphy could be
115 identified. In the latter case, samples were only collected where flints were still surrounded
116 with thick chalk deposits that were assumed to protect the flint from impact damage. Some of
117 the flint blocks from the different sites are shown in Figure 3 and description of flint samples
118 are provided below.

119

120 *Flints from the Burnham Chalk, North Landing, Yorkshire, United Kingdom.*

121 The flint samples from the North Landing, UK are tabular, mostly grey (Figs. 3a, and b)
122 and highly fractured (Fig. 3c, both macro/microfractures). Fracturing in these samples might
123 be associated with tectonic activity as the collection site is near the Flamborough Head faults.
124 The North Landing flint has a white crust (Fig. 3a) which commonly exceeds 20 mm
125 thickness, and is stronger than the surrounding chalk, but weaker than the enclosed flint core.
126 These flint samples have higher calcite content than other flints. Most of these flint samples

127 are up to 300 mm thick and comprise significant quantities of partially silicified carbonate
128 inclusions (Fig. 3b) and in some cases most of the sample is dominated by the light grey flint.
129 Brownish grey flints are also found in the North Landing Chalk with significant quantities of
130 calcite inclusions (Fig. 3b).

131

132 *Flints from the Anglo-Paris Basin, United Kingdom and France.*

133 The flints in the Anglo-Paris Basin chalk are shown in Figure 3d-f. Figure 3d is a flint
134 from the Seaford Chalk, East Sussex, UK, Figure 3e is a flint in the Seaford Chalk, Dieppe,
135 France and Figure 3f is a flint in the Lewes Nodular Chalk, Mesnil-Val, France. These flint
136 samples are mostly dark brownish grey, with a few silicified inclusions. These inclusions
137 appear as light brownish grey irregular shaped zones in the samples. The dark brownish grey
138 flints appeared more competent than the grey flints. Microfractures are rarely seen in these
139 flints, and the white crust surrounding the dark brownish grey flints are thinner and harder
140 when compared with those surrounding the grey flints from the Burnham Chalk Formation.

141 *Geology of the Study Sites*

142 The geology at North Landing is described in Mortimore *et al.* (2001). The Burnham
143 Chalk Formation (Turonian-Santonian, see Fig. 4) includes the entire *Sternotaxis plana* zone
144 to the lower part of the *Micraster cortestudinarium* zone. The Formation overlies the Welton
145 Chalk Formation and is overlain by the Flamborough Chalk Formation. It is characterised by
146 the tabular flints ($\geq 0.3\text{m}$ thick) (Wood & Smith 1978; Gale & Rutter 2006), Paramoudra and
147 semi-tabular flints. It comprises thinly bedded chalk with flints and is 130-150 m thick in this
148 area (Mortimore *et al.* 2001; Hopson 2005). The base of this formation has more flint bands
149 than other parts of the formation (Wood & Smith 1978) and is characterised by conspicuous
150 layers of light grey, highly fractured carious tabular flints.

151 The geology of the chalk at the sites sampled in the Anglo-Paris Basin is described by
152 Mortimore *et al.* (2001) and Bristow *et al.* (1997). The Seaford Chalk Formation (middle
153 Coniacian-middle Santonian, see Fig. 4) is described in Mortimore (1986); Mortimore &
154 Pomerol (1997); Bristow *et al.* (1997) and Mortimore *et al.* (2001). The formation is composed
155 of pure (>98%) calcium carbonate, very weak, white, fine-grained chalk, with extensive bands
156 of dark nodular flints and sheet flints can also be commonly found in this formation. The
157 formation is bound at the top by marl seams and by the basal marker the Shoreham Marl. The
158 formation also includes the Seven Sisters Flint which is a conspicuous marker bed and is also
159 traceable along the French coast (Upper-Normandy and Picardy) (Mortimore *et al.* 1986).

160 The French sampling site at Mesnil-Val in Picardy, is a coastal cliff section composed
161 of the Lewes Nodular Chalk Formation (Upper Turonian-Lower Coniacian stage, see Fig. 4)
162 as described in Mortimore *et al.* (2001). The Lewes Chalk Formation comprises marl seams,
163 and well bedded, nodular chalk with nodular flint bands. These flint bands are parallel to the
164 bedding, laterally extensive and traceable in the stratigraphy (Mortimore 1986; Mortimore &
165 Pomerol 1987; Busby *et al.* 2004; Senfaute *et al.* 2009). Apart from nodular flint bands, tubular
166 and semi-tabular flints are also present in places along the chalk cliff section.

167 *Sample description*

168 The flint samples are initially classified on the basis of the geological features, mainly
169 body colour characteristics (Figs. 3a-f and 5). The flint colour classification is based on
170 Munsell colour chart as given in Table 1. The frequently used notations representing flint types,
171 geological units and geographical locations are provided in Table 2. Flint samples were tested
172 at their natural moisture content and at laboratory temperature. The test method and typical
173 sample sizes used for the geomechanical tests are provided in Tables 3 and 4 respectively.

174 *Microstructure and mineralogical Characterisation*

175 The external morphology, grain shape, orientation and degree of
176 crystallisation/cementation of the flint are characterised using scanning electron microscopy
177 (SEM) to aid in explaining the physical and mechanical properties of flints. The mineralogy,
178 including the silica phases, is assessed using XRD.

179 *Scanning Electron Microscope*

180 SEM analysis, including secondary electron images (SEI) was conducted on samples
181 with size of approximately 10 x 10 x 5 mm. The analysis was conducted on twelve flint samples
182 selected to be representative of the various flint classes (Fig. 5). These were coated with gold
183 in a BIO-RAD-SC500 Sputter coater for 4 – 5 minutes to inhibit the concentration of electrical
184 charge on the samples. The coated samples were analysed using a JEOL-JSM-6610LV SEM
185 machine equipped with an Oxford Instrument Energy Dispersive X-rays (EDX) detection
186 analyser, which is used to identify and quantify mineral phases of the samples. Images were
187 captured using an accelerating voltage of 15 keV.

188 *X-Ray Diffraction*

189 XRD analysis was carried out using a Bruker D8 XRD instrument, it was performed on
190 flint specimens similar to those characterised using the SEM. These samples were ground into

191 powder and pressed into a mount in order to produce a randomly oriented powder. The mounts
192 were analysed in turn. A Cu α radiation source was used. The specimens were scanned over
193 an angular range of 2-90° 2 θ , with a step size of 0.01°. The data were processed using Bruker
194 EVA search match software for phase identification while Bruker TOPAS profile and structure
195 analysis software were used to quantify the mineral phases present.

196 *Geomechanical Properties Tests*

197 The methods used for testing samples are outlined in Table 3 and the geometry of tested
198 samples reported in Table 4. The majority of these methods use standard test procedures.
199 Deviations from the standard method will be discussed. Two testing machines were used. These
200 were the MAND Universal Compression Testing Machine (250 kN capacity with a precision
201 0.1 kN) for the tensile testing and the Denison compression machine (capacity of 2000 kN with
202 precision of 0.05 kN) for compression testing.

203 *Bulk density (ρ)*

204 The bulk density (ρ) of flint was determined using the caliper method. The bulk mass of each
205 specimen was measured using a digital scale. The bulk volume was obtained from the mean of
206 five readings for each dimension taken at various points of the specimens. Bulk density was
207 calculated from the relationship between the bulk mass and the bulk volume of each flint
208 specimen (Equation 1).

$$210 \quad \rho = \frac{\text{bulk mass } (M_b)}{\text{bulk volume } (v_b)} \text{ ————— (1)}$$

211 Where: ρ is the bulk density (Mg m^{-3})

212 *Tensile strength (T_o)*

213 For the tensile strength (T_o), the Three-point beam method described by Brook (1993)
214 was used to determine the tensile strength of flint by bending. The test was developed to
215 estimate tensile strength by subjecting samples to stress by applying steady central load
216 between two ball bearings until the samples fail by bending. The positioning of the bearings is
217 dictated by sample length. The concentrated load applied to the sample causes tensile
218 deformation along the point of the applied load, which leads to a tensile failure.

219 The Three-point beam method was used instead of the direct tensile test and the Brazil
220 test because:

- 221 1) Less sample preparation and no surface finish was required;

223 2) Smooth or flat ends were not required.

224 These requirements mean that a beam of flint can be more easily prepared and tested using this
225 method than the standard disc required for the Brazil test or the direct tensile test. The tensile
226 strength derived from beam method was found to compare well with that of direct pull test
227 (Brook 1993) and with tensile strength obtained from the Brazilian test for flint (Cumming
228 1999). The Three-point-beam test was carried out using the MAND universal compression
229 testing machine. Tensile strength was calculated using Equations 2 and 3.

230

231
$$T_0 = \frac{P}{G} \text{-----} (2)$$

232
$$G = \frac{4bd^2}{3l} \text{-----} (3)$$

233

234 Where: T_0 is the tensile strength (MPa), P is the failure load (kN), G is the geometry factor, b
235 is the breadth of the sample (mm), d is the thickness of the sample (mm), l is the span between
236 the ball bearings.

237

238 *Point Load Strength Test*

239 Point load strength index ($I_{s(50)}$) of flint was measured on an ELE International point load
240 machine with a loading capacity of 56 kN and a precision of 0.05 N. Both blocks and irregular
241 specimens were tested in accordance with ISRM (2007) suggested methods. The dimensions
242 of the specimens range from length=25-90 mm, width=19-45 mm, and diameter=15- 44 mm.
243 Sample geometry was constrained by challenges of preparing flint samples. The samples sizes
244 used were within the 50 ± 35 mm tolerances contained in the suggested method. Samples were
245 tested at a loading rate resulting in failure between 10-60 seconds after the start of the test. The
246 failure loads were then recorded, the $I_{s(50)}$ for each specimen was calculated using Equations 4
247 to 9 (ISRM 2007).

248

249
$$A = W \times D \text{-----} (4)$$

250

251
$$De^2 = \frac{4D}{\pi} \text{-----} (5)$$

252

253
$$De = \sqrt{De^2} \text{-----} (6)$$

254

255
$$I_s = \frac{(P \times 1000)}{De^2} \text{-----} (7)$$

256

257
$$F = \left(\frac{De}{50}\right)^{0.45} \text{-----} (8)$$

258

259
$$I_{s50} = F \times I_s \text{-----} (9)$$

260

261 Where: A is the minimum cross sectional area of the point of contact for the loading platens on
 262 the sample (mm^2), De is the equivalent sample diameter (mm), F is the Size correction factor,
 263 I_s is the Uncorrected Point load strength index (MPa), and $I_{s(50)}$ is the corrected Point load strength
 264 index (MPa).

265

266 *Uniaxial Compressive Strength (UCS) Test*

267 Uniaxial compressive strength (UCS) of flint was measured using Denison machine with
 268 the capacity of 2000 kN at loading rate of 0.5 MPas^{-1} . The machine has an accuracy of 0.05
 269 kN. The test was conducted on both cores and cuboid flint specimens in accordance with ASTM
 270 D2845 2000; ISRM 2007; ASTM D7012-07 2010 suggested methods. A typical sample size
 271 of 25 mm diameter was used. The choice of this size was informed by the repeated failure of
 272 attempts to produce cylindrical core samples of NX size (54 mm). The cuboid flint specimens
 273 were only prepared for the flint samples from the Burnham Chalk Formation due to difficulty
 274 in preparing cylindrical samples because of fractures/joints and carbonate inclusions in the
 275 samples.

276

277 *Young's modulus and Poisson's ratio*

278 The deformability (Young's modulus and Poisson's ratio) of flint specimens was determined
 279 in accordance to ISRM 2007 suggested methods from the strain measurements. Strain was
 280 measured using 5 mm electrical resistance strain gauges. The axial stresses, axial, and lateral
 281 strains, were recorded using a windmill logger. These data were used to plot stress-strain curves
 282 from which elastic properties comprising static Young's modulus (E_s), and static Poisson's
 283 ratio (ν_s) were determined. The average method was used to determine the E_s of flint using
 284 Equation 10. This involves deriving E_s from the approximate linear part of the axial stress-
 285 strain curve (ISRM 2007). The ν_s was then calculated from the relationship between E_s and the
 286 slope of diametric curve using Equation 11.

287 The deformability of all the investigated flint specimens was measured except the flint
288 specimens from the Burnham Chalk Formation. The deformability of these specimens was not
289 measured because the strain gauges detached from the specimens at early stage of loading due
290 to spalling of the flints under load. The spalling of these flints was likely associated with
291 closely spaced (c. 10 – 15 mm) orthogonal incipient fractures in the specimens.

292
293

$$294 \quad E_s = \frac{\Delta \text{Axial stress}}{\Delta \text{Axial strain}} \text{-----} (10)$$

295

$$296 \quad v_s = \frac{E_s}{\text{Slope of diametral curve}} \text{-----} (11)$$

297

298 The physical and mechanical properties were subjected to statistical analysis using One-
299 way ANOVA and Post-Hoc tests using Tukey's test. The One-way ANOVA was used because
300 normality test using the Shapiro-Wilk shows most of the data was drawn from normally
301 distributed population (Table 5) except in four cases where normality was rejected (bold in
302 Table 5). In the four cases, two have about 50 specimens in which case normality can be
303 assumed due to large sample size in the population. The two remaining cases E_s for SDFr and
304 T_o for LMFr (both in Table 5) were treated as non-normally distributed data. Thus, to check
305 the influence of distributions of data, both parametric and non-parametric statistics were used
306 to analyse the overall results (summarised in Tables 6 and 7).

307 **Results**

308 *Petrographic Observations*

309 The principal minerals identified in all the flint samples investigated were α -quartz and
310 calcite, the percentages of which vary with flint structure and geographic locations (Table 5).
311 A summary of the mineralogy of different flint structures and class by location is given in Table
312 8.

313 In the white crusts of the Burnham Chalk Formation, granular, flaky calcite crystals
314 with clusters of quartz microspheres and traces of cryptocrystalline quartz are evident
315 (BNLUK, Fig. 6a).

316 The white crust of the Seaford Chalk from both sites have a homogeneous phase
317 dominated by cryptocrystalline quartz (Figs. 6a-c). The recrystallisation of quartz grains into

318 massive quartz cements is apparent in the white crust (WCr) of the Seaford Chalk Formation
319 Dieppe, France (Fig. 6c). The WCr from both Seaford Chalk Formations are relatively more
320 cemented than those from BNLUK and have amorphous silica particles (enclosed in white in
321 Figs 6b & c) with some clusters of quartz microspherules (indicated by the arrows in Fig. 6c).

322 Spherical quartz grains that have transformed into clusters of quartz microspheres are
323 seen in the light brown grey, brown grey and grey flints of the Burnham Chalk (Figs. 6d, h,
324 and l). Quartz cements also occur intermittently in these samples and are also observed in the
325 light brownish grey flints (Fig 6. e-g). The clusters of quartz microspheres are more pronounced
326 in the GF (Fig. 6l) from the Burnham Chalk Formation, North Landing, UK (BNLUK) than
327 light brownish grey flints from the same chalk formation. Spherical quartz grains with
328 interparticle pores and microfractures are seen in the LBG of the BNLUK samples (white
329 arrows in Fig. 6d). These interparticle microfractures are also evident in the BG flint of the
330 BNLUK category.

331 The LBG and DBG flints in the Seaford Chalk at East Sussex, (SESUK), Seaford Chalk
332 at Dieppe, France (SDFr) and Lewes Chalk Mesnil-Val, France, (LMFr) appeared distinct
333 (Figs. 6i-k). These flint samples exhibit networks of massive quartz cements forming
334 agglomeration of quartz grains/flakes and cements (Fig. 6k). These flint types show greater
335 cementation compared to those of GF (BNLUK).

336 ***Mechanical Properties by Location***

337 The results of the mechanical properties of flints are expressed as box and whisker plots Figure
338 7. The main statistical analysis of the results is given in Tables 6 and 7 presented according to
339 locations and geological units which vary with flint class. Box and Whiskers are used to show
340 the overall distribution of the results. Cross plots are used to show the influence of sample sizes
341 on strength of flints and the distribution of some engineering geological parameters.

342 Figures 7a-d show data for the flints obtained from North Landing and the Anglo-Paris
343 Basin. It can be seen that by comparison to flints from the south of England and France, are
344 denser than those from North Landing (mean density 2.42 Mgm^{-3} as opposed to $2.66\text{-}2.69$
345 Mgm^{-3}). This tends to suggest a lower degree of silicification (see Fig. 6a) than in the flints
346 found within the Southern Province chalk. Concurrently, it is therefore unsurprising that T_c ,
347 UCS and $I_{s(50)}$ for the North Landing flints are significantly lower than those from elsewhere.
348 In 7b, c and d, it is clear that the flints from the Anglo-Paris Basin (extracted from the Seaford
349 and Lewes Chalk formations) show a range of mechanical properties which are broadly similar.
350 Equally, as can be seen in 7e and 7f, Young's Modulus and Poisson's Ratio for flint samples

351 extracted from the English and French sites are broadly similar. While it can be seen that there
352 is some overlap in the natural material variation, the overlap is small (Tables 6 and 7).

353 ***Tensile Strength (T_o)***

354 Figure 7b shows results of variations in tensile strength (T_o) as summarised in Tables 6
355 and 7. Flints in the Burnham Chalk Formation, North (BNLUK) generally show the lowest
356 mean and ranges of tensile strength compared with those of Seaford and Lewes Chalk
357 Formations. In some specimens of the BNLUK flints a weak correlation between tensile
358 strength and carbonate content was observed. This correlation is indicated by the absence of
359 the two major data point cluster (observed in Figs. 7c and d) exhibiting differences in strength
360 between samples with higher calcite inclusions and samples with lower calcite inclusions. The
361 T_o values for samples from the Seaford and Lewes Chalk formations were all greater than those
362 for the Burnham Chalk Formation and were similar (in both the mean and median values, Table
363 6).

364 ***Point Load Strength Index ($I_{s(50)}$)***

365 A similar pattern to that seen during the tensile testing program was observed during the
366 point load strength index testing. The plot of $I_{s(50)}$ for the four flint types is provided in Figure
367 7c. Again, the $I_{s(50)}$ values for flints from the Burnham Chalk are distinctly lower than those
368 from other locations. The recorded values of $I_{s(50)}$ were in the range of 3.07-12.31 MPa flint in
369 the Burnham Chalk Formation, North (BNLUK). A comparison of the $I_{s(50)}$ values between
370 dark brownish grey flints in the Seaford Chalk Formation at East Sussex, UK, Dieppe, France
371 and flints in the Lewes Chalk Formation does not show any significant differences (Tables 6
372 and 7) even between the results of parametric and non-parametric statistics.

373 ***Uniaxial Compressive Strength***

374 The UCS of the flints studied is shown in Figure 7d and the statistical observations are
375 presented in Tables 6 and 7. It should be noted that in both statistical approaches employed,
376 grey flints in the Burnham Chalk, North Landing (BNLUK) consistently remain the weakest
377 material as against the stronger, dark brownish grey flints from other formations. This is
378 consistent with the trends in T_o and $I_{s(50)}$ results. The UCS of flints in the Seaford Chalk
379 Formation at East Sussex, Dieppe, France and for flints in the Lewes Chalk Formation
380 corresponds to the extremely strong category. However, a significant difference exists in the
381 UCS of the flints from Burnham Chalk Formation forming two major clusters with mean UCS

382 and standard deviation as low as 112.2 ± 71.0 MPa within a range of 25.2 to 232.4 MPa were
383 recorded. The wide range observed in these samples is associated with calcite inclusions and
384 microfracturing in the samples.

385 In order to define the deformation characteristics of flints, elastic properties comprising
386 Young's modulus (E_s), and static Poisson's ratio (ν_s) were determined (Figs. 7e and f) and
387 Tables 7 and 8 provides the summary of the overall results. The E_s ranges, mean and standard
388 deviation values for flints in the Seaford Chalk Formation from East Sussex and from Dieppe
389 and flints in the Lewes Chalk Formation indicate these flints are extremely stiff, with very
390 slight variation in stiffness among the samples (Tables 6 and 7). As observed in all the
391 mechanical tests, the ν_s for the dark brownish grey flints from the Seaford and Lewes Chalk
392 Formations representing the three respective sites were similar (Fig. 7f and summarised in
393 Tables 6 and 7). These ν_s values range from 0.050-0.181 and the overall data points mimicked
394 the heterogeneity within the individual flint specimens characterised by the presence of
395 partially silicified inclusions and minor variations in mineral composition.

396 **Discussion**

397 *General observations*

398 The characterisation of flints reported in this paper focused on both physical and
399 mechanical properties of flints and relate these with the petrographic observations to
400 understand how the behaviour of flints is shaped by the mineralogy and microfractures. Due to
401 the different tectonic setting of each site an investigation into the effects this has on the geo-
402 mechanical properties of the flint was possible.

403 The results of physical and mechanical investigations (summarised in Tables 6 and 7)
404 indicate that the engineering properties of flints vary with flint class. The relationship between
405 ρ and UCS is presented in Figure 8. The effects of sample sizes on the overall strength results
406 assessed from the cross plots of strength and sample sizes (Figs 9a and b; Fig. 10) suggest that
407 variations in sample sizes do not affect the present findings as there was no observed clear
408 relationship in the cross plots.

409 The results of density measurements, tensile and compressive strength tests and point
410 load strength index tests (I_{s50}) are shown in Figures 7. The results from the mechanical tests
411 show considerable variation in flint strengths which is consistent with other studies (e.g.
412 Cumming 1999; Mortimore *et al.* 2011; Smith *et al.* 2003) as shown in Table 9 which highlights
413 previous studies and shows the variation in the results.

414 If flints are classified into dark brown-grey flints (DBG) and grey flints (GF), it is
415 generally observed that the densest, strongest and stiffest materials fall into the DBG category.
416 This is consistent with the mineralogical observations which show that in that DBG flints have
417 the highest silica content over 99% regardless of location (Table 8). So in general at any given
418 location the higher silica content (and correspondingly lower calcite content) leads to the
419 densest, strongest and stiffest flints.

420

421 *The Burnham Conundrum*

422 Even at the stage of sample preparation and field observation it was apparent that the
423 flints sampled from the Burnham Chalk at Flamborough Head were significantly different from
424 those observed in the chalk of the Anglo-Paris Basin. This difference is characterised by the
425 presence of centimetre scale fractures in the flint (Fig. 1a). These tend to form in a bedding-
426 parallel orientation and at 90° to bedding. This has led to two possibilities: (i) the flints in the
427 Burnham Chalk are fractured or (ii) the flints at Flamborough Head are fractured. The higher
428 calcite content observed could explain the weaker strength properties of these flints, but not
429 the presence of the fracturing. These flints showed less cement and possessed larger, more
430 spherical quartz grains compared with other flints (see SEM images Figs. 6a-l).

431 In order to investigate these hypotheses grey flints from the Burnham Chalk Formation
432 were collected in Lincolnshire (mean UCS=310 MPa, mean ρ =2.49 gcm⁻³). These flints do not
433 contain similar centimetre scale fractures and so it is most likely that the Burnham Chalk flints
434 at North Landing have been intensely fractured because of the complex tectonic structures
435 related to faulting such as those seen in Selwick Bay (TA 205 687) less than 2 km to the south
436 east where major a fault complex of normal and reverse faults related to east-west faulting and
437 folding movements initiated as frontal movements from the offshore Dowsing Fault
438 (Mortimore *et al.*, 2001). In the chalk itself, this movement is readily accommodated via layer
439 parallel slip, whereas for the more brittle flints shearing and fracturing due to the large stiffness
440 differences is the only available mechanical option. This tends to confirm the postulated effects
441 of tectonics on the strength of flints from the Southern Province of the UK suggested by
442 Cumming (1999). It seems likely that this is an effect associated with extensional tectonism
443 rather than compressional since the extremely high compressive strengths of flint are unlikely
444 to allow brittle compression fracture to develop.

445

446 *Mineralogical controls on mechanical properties.*

447 The main mineralogical control on the mechanical properties of flint is the percentage
448 of silica within the sample. The colours of flints generally reflect the silica-calcite ratios within
449 the rock. Although some halite was observed on XRD traces, this is believed to be
450 contamination from sea spray. Generally there is an increase in the quartz content from the
451 white crust through the light brown grey; brownish grey; grey flint and into the dark brown
452 grey flints (Table 8). There is conversely an increase in the carbonate content.

453 The evidence of high sphericity of quartz grains and interparticle voids in the weaker,
454 less dense grey flints compared to the stronger, denser, intensely silicified micro fabrics of the
455 dark brownish grey flint supports the hypothesis that the microtexture and the microstructure
456 of flint exert significant control on the engineering behaviour of flint (Tables 6-8). Figure 8
457 shows that the highly cemented/silicified dark brownish grey flints showed significantly higher
458 strength and density than the predominantly grey flints. There is some natural scatter which is
459 a function of natural variability of the flint materials. Density can be used as a proxy to strength
460 for example the more siliceous dark brownish grey flints were observed to be denser and
461 stronger compared to the less siliceous grey flints as shown in Figure 8.

462 Reported values of Young's Modulus show small variations from previously reported
463 observations (Pabst & Gregorová 2013). However, it is likely that such variations fall within
464 the range of uncertainty of natural materials and can be attributed to observational bias due to
465 different techniques being used in the measurement. Similarly, measured Poisson's ratio (ν_s)
466 of flint samples from the Seaford Chalk and Lewes Chalk Formations are broadly consistent
467 with the results of Gercek (2007).

468 **Summary and Conclusions**

469 An investigation of three groups of flints from the United Kingdom and France is reported.
470 Significant differences in the mechanical properties of flints exist.

471 The principle control on the mechanical properties of flint is the relative proportions of
472 quartz to calcite in the rock. Such proportions also control the colour of the materials and
473 therefore it is possible to classify flints on the basis of colour. The observed colour ranges from
474 the white crust (often found around flints), which is in effect a highly silicified chalk, through
475 to the dark brown grey flints with the lowest percentage of calcium carbonate. Given the
476 empirical relationship between abrasivity and quartz content, colour may be a useful predictor
477 of potential abrasivity at the desk study stage approach of a site investigation. Further
478 investigation is required to confirm the validity of this relationship outside the Anglo-Paris
479 Basin.

480 It is observed that the flints found in the Burnham Chalk Formation from North Landing
481 in Yorkshire show lower densities and lower strength properties than other materials. The dark
482 brownish grey flints in the Seaford and Lewes Formations have similar strength values
483 supporting the view that colour is a useful predictor regardless of geographic location and
484 stratigraphic control. The fracturing in the flints found at North Landing is likely to be a
485 tectonic effect and the potential for such fracturing should be considered during site
486 investigations in the proximity of large extensional faults. Further research is required to clarify
487 whether such effects exist for compressional tectonic environments given the significantly
488 higher strength of flints in compression.

489

490 **Acknowledgement**

491 This research project is funded through a doctoral training award from the Petroleum
492 Technology Development Fund (PTDF), Nigeria. The American Association of Petroleum
493 Geologists is acknowledged for supporting part of the French fieldwork. Mr Kirk Handley and
494 Dr John Martin are acknowledged for assistance in geotechnical testing. Dr. Algy Kazlauciusas
495 and Lesley Neve assisted with SEM and XRD analyses respectively. The encouragement and
496 advice of two anonymous reviewers is gratefully acknowledged.

497 **References**

- 498 ASTM 2000. *Standard test method for laboratory determination of pulse velocities and*
499 *ultrasonic elastic constants of rock (D2845-00)*. West Conshohocken, American
500 Society for Testing Materials, ASTM.
- 501 ASTM 2010. *Standard test method for compressive strength and elastic moduli of intact rock*
502 *core specimens under varying states of stress and temperatures (D7012)*. Philadelphia,
503 American Society for testing materials, ASTM.
- 504 BRISTOW, C. R., MORTIMORE, R. N. & WOOD, C.J. 1997. Lithostratigraphy for mapping
505 the Chalk of southern England. *Proceedings of the Geologists' Association*, **108** (4),
506 293-315.
- 507 BROCH, E. & FRANKLIN, J. A. 1972. The point-load strength test. *International Journal*
508 *of Rock Mechanics and Mining Sciences & Geomechanics*. **9** (6), 669-676. Pergamon.
- 509 BROMLEY, R. G. 1967. Some observations on burrows of Thalassinoidean Crustacea in
510 chalk hardgrounds. *Quarterly Journal of the Geological Society*, **123**, 157- 177.
- 511 BROMLEY, R. G., SCHULZ, M. G. & PEAKE, N. B. 1975. Paramoudras: giant flints, long
512 burrows and the early diagenesis of chalks. *Kongelige Danske Videnskabernes*
513 *Selskab Biologiske Skrifter (Biological Series)*, **20** (10), 31.
- 514 BROOK, N. 1993. The measurement and estimation of basic rock strength. *Comprehensive*
515 *rock engineering*, **3**, 41-66.
- 516 BUSBY, J. P., SENFAUTE, G., GOURRY, J. C., LAWRENCE, J. A., PEDERSON, S. A. S.
517 & MORTIMORE, R. N. 2004. Developing tools for the prediction of catastrophic
518 coastal cliff collapse. *In: Proceedings of the 7th International Symposium – Delivering*
519 *Sustainable Coasts: Connecting Science and Policy*, Aberdeen, Scotland, UK, 2004,
520 596–601.
- 521 CLAYTON, C. J. 1986. The chemical environment of flint formation in Upper Cretaceous
522 chalks. *In: SIEVEING, DE G. & HART, M. B. (eds) The scientific study of flint and*
523 *chert*. Cambridge University Press, Cambridge, 43-53.
- 524 CLAYTON, C. J. 1984. *The geochemistry of chert formation in Upper Cretaceous chalks*.
525 Unpublished PhD Thesis, King's College London (University of London).
- 526 CUMMING, F. M. D. F. 1999. *Machine tunnelling in chalk with flint with particular reference*
527 *to the mechanical properties of flint*. Unpublished PhD Thesis, University of Brighton.
- 528 DOMAŃSKI, M. & WEBB, J. A. 2000. Flaking properties, petrology and use of Polish flint.
529 *Antiquity*, **74** (286), 822-832.

- 530 GALE, I. N. & RUTTER, H. K. 2006. The chalk aquifer of Yorkshire: Keyworth: British
531 Geological Survey. *Research Report*, RR/06/04, 1-62.
- 532 GERCEK, H. 2007. Poisson's ratio values for rocks. *International Journal of Rock Mechanics
533 and Mining Sciences*, **44** (1), 1-13.
- 534 GRAETSCH, H. A. & GRÜNBERG, J. M. 2012. Microstructure of flint and other chert raw
535 materials. *Archaeometry*, **54** (1), 18–36.
- 536 HOPSON, P. 2005. *A stratigraphical framework for the Upper Cretaceous Chalk of England
537 and Scotland with statements on the Chalk of Northern Ireland and the UK Offshore
538 Sector*. British Geological Survey Research Report No. RR/05/01.
- 539 HUGHES, R. E., HÖGBERG, A. & OLAUSSON, D. 2012. The Chemical Composition of
540 Some Archaeologically Significant Flint from Denmark and Sweden. *Archaeometry*,
541 **54** (5), 779-795.
- 542 HUGHES, R. E., HÖGBERG, A. & OLAUSSON, D. 2010. Sourcing flint from Sweden and
543 Denmark. *Journal of Nordic Archaeological Science*, **17**, 15-25.
- 544 ILER, R. K. 1963. Strength and structure of flint: *Nature*, **4900**, 1278-1279.
- 545 ISRM, 2007. *The complete ISRM suggested methods for rock characterization, testing and
546 monitoring: 1974-2006*: In Ulusay, R., & Hudson, J. A. (eds) Suggested methods
547 prepared by the commission on testing methods, International Society for Rock
548 Mechanics, Commission on Testing Methods (ISRM Turkish National Group).
- 549 JAKOBSEN, F., LINDGREEN, H. & NYTOFT, H. 2014. Oil-impregnated flint in Danian
550 Chalk in the Tyra Field, North Sea Central Graben. *Journal of Petroleum Geology*, **37**
551 (1), 43-53.
- 552 JEANS, C. V. 1978. Silicifications and associated clay assemblages in the Cretaceous marine
553 sediments of southern England. *Clay Minerals*, **13** (1), 101-126.
- 554 MADSEN, H. B., STEMMERIK, L. & SURLYK, F. 2010. Diagenesis of silica-rich mound-
555 bedded chalk, the Coniacian Arnager Limestone, Denmark. *Sedimentary Geology*, **223**
556 (1-2), 51–60.
- 557 MORTIMORE, R. N. 1986. Stratigraphy of the Upper Cretaceous White Chalk of Sussex.
558 *Proceedings of the Geologists' Association*, **97** (2), 97-139.
- 559 MORTIMORE, R. N. 2011. A chalk revolution: what have we done to the Chalk of England?
560 *Proceedings of the Geologists' Association*, **122** (2), 232-297.

- 561 MORTIMORE, R. 2012. Making sense of Chalk: a total-rock approach to its Engineering
562 Geology. *Quarterly Journal of Engineering Geology and Hydrogeology*, **45**(3), pp.252-
563 334.
- 564 MORTIMORE, R. N., NEWMAN, T., ROYSE, K., SCHOLE, H. & LAWRENCE, U. 2011.
565 Chalk: its stratigraphy, structure and engineering geology in east London and the
566 Thames Gateway. *Quarterly Journal of Engineering Geology and Hydrogeology*, **44**
567 (4), 419-444.
- 568 MORTIMORE, R. N. & POMEROL, B. 1997. Upper Cretaceous tectonic phases and end
569 Cretaceous inversion in the Chalk of the Anglo-Paris Basin. *Proceedings of the*
570 *Geologists' Association*, **108** (3), 231-255.
- 571 MORTIMORE, R. N., WOOD, C.J. & GALLOIS, R. W. 2001. *British upper Cretaceous*
572 *stratigraphy*, Geological Conservation Review Series, No. 23, Joint Nature
573 Conservation Committee, Peterborough, 558 pp.
- 574 OLAUSSON, D., HUGHES, R. E. & HÖGBERG, A. 2012. Provenance studies on
575 Scandinavian Flint. *Acta Archaeologica*, **83** (1), 83-86.
- 576 PABST, W. & GREGOROVÁ, E. 2013. Elastic properties of silica polymorphs—a review
577 *Ceramics-Silikaty*, **57**, 167.
- 578 PRADEL, L. & TOURENQ, C. 1967. Les matériaux de Fontmaure Choix des Paléolithiques
579 et mesures des caractères physiques. *Bulletin de la Société préhistorique française.*
580 *Comptes rendus des séances mensuelles*, LXXXI-LXXXV.
- 581 PRADEL, L. & TOURENQ, C. 1972. Choix des matériaux par les Paléolithiques de Fontmaure
582 et essais de fragmentation dynamique. *Bulletin de la Société préhistorique française.*
583 *Comptes rendus des séances mensuelles*, **69** (1), 12-12.
- 584 PRUDÊNCIO, M. I., ROLDÁN, C., DIAS, M. I., MARQUES, R., EIXEA, A. &
585 VILLAVARDE, V. 2015. A micro-invasive approach using INAA for new insights into
586 Palaeolithic flint archaeological artefacts. *Journal of Radioanalytical and Nuclear*
587 *Chemistry*, **308**, 1-9.
- 588 SENFAUTE, G., DUPERRET, A. & LAWRENCE, J. A. 2009. Micro-seismic precursory
589 cracks prior to rock-fall on coastal chalk cliffs: a case study at Mesnil-Val, Normandie,
590 NW France. *Natural Hazards and Earth System Science*, **9** (5), 1625-1641.
- 591 SMITH, N. A., HISLAM, J. L. & FOWELL, R. J. 2003. A Note On the Strength of Flint
592 Particles. In: Handley, M. & Stacey, R. *Technology roadmap for rock mechanics*. South
593 African Institute of Mining and Metallurgy, **2**, 1105-1108.

- 594 VARLEY, P.M. 1990. Machine excavation of chalk rock at the first South
595 Killingholme gas cavern, South Humberside. *In*: Burland, J.B., Mortimore,
596 R.N., Roberts, L.D., Jones, D.L. & Corbett, B.O. (eds) *Chalk. Proceedings of the*
597 *International Chalk Symposium, Brighton Polytechnic, 1989*. Thomas
598 Telford, London, 485–492.
- 599 WASHBURN, E. W. & NAVIAS, L. (1922). The relation of chalcedony to other forms of
600 silica. *Proceeding of the National Academy of Sciences of the United States of America*, **8** (1),
601 1.
- 602 WASILEWSKI, M. 2002. Mineralogical investigation of desert patina on flint artifacts: A case
603 study. *Mediterranean Archaeology and Archaeometry*, **2** (2), 23-34.
- 604 WEYMOUTH, J. H. & WILLIAMSON, W. O. (1951). "Some physical properties of raw and
605 calcined flint". *Mineralogical Magazine*, **29** (213), 573-593.
- 606 WOOD, C. J. & SMITH, E. G. 1978. Lithostratigraphical classification of the chalk in North
607 Yorkshire, Humberside and Lincolnshire. *Proceedings of the Yorkshire Geological*
608 *Society*, **42**, 263-287.
- 609

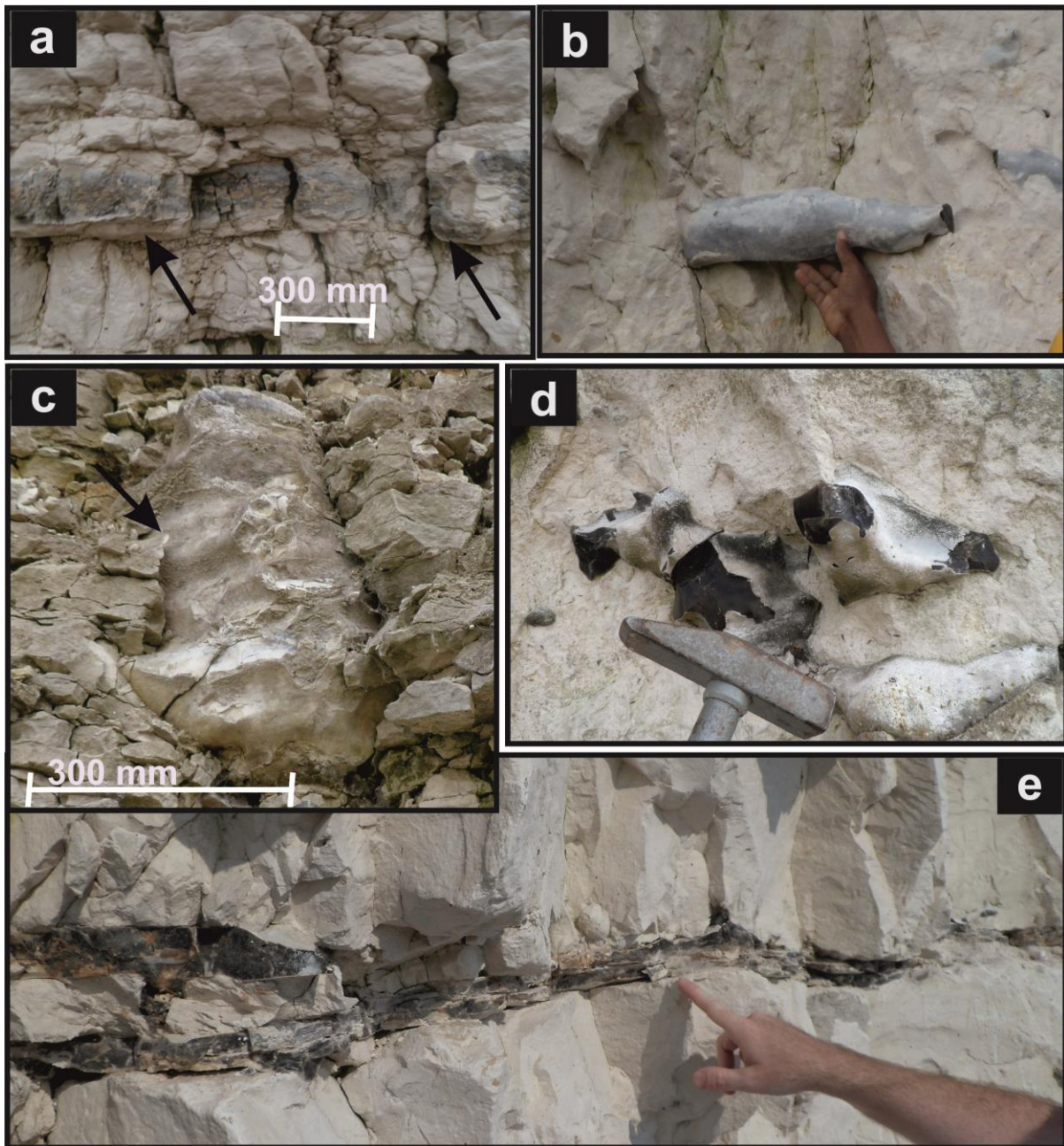


Fig. 1. (a) Tabular Flint in Burnham Chalk Formation, North Landing, UK ; (b) Tubular Flint, Lewes Chalk Formation, France; (c) Paramoudra Flint, Burnham Chalk Formation, Ucerby Vale Quarry, Lincolnshire, UK; (d) Nodular Flint, Seaford Chalk Formation, East UK; Sussex, (e) Sheet Flint, Seaford Chalk Formation, East Sussex, UK.

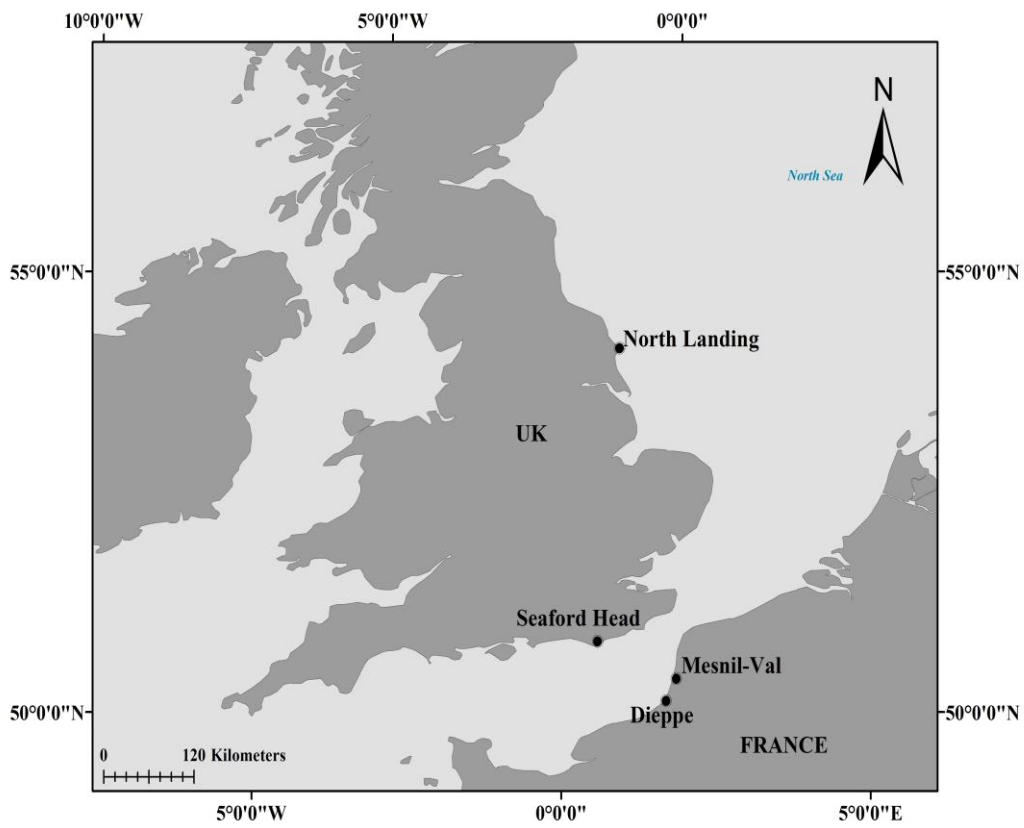


Fig. 2. Map of UK and north western France with the study locations highlighted.

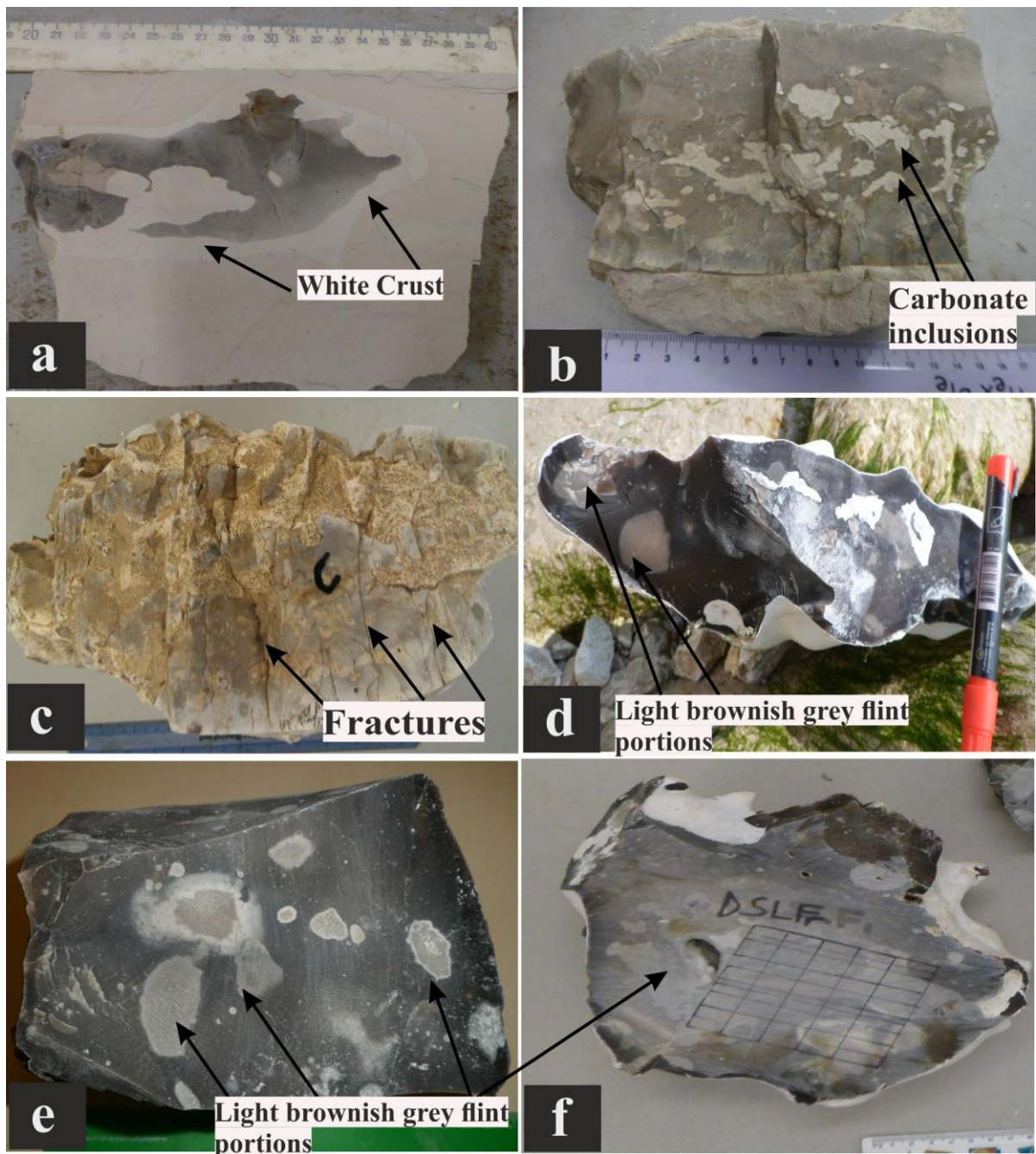


Fig. 3. (a-f) Flint Blocks from the four (4) study sites showing different structures and colours of flint. (a-c) Represent flint blocks from the North Landing, UK. Note the white crust in (a), brownish grey flint with white inclusions in (b), and highly fractured grey flint in (c). (d, e and f) Dark brown flint from Seaford Chalk, UK, France and Lewes Chalk, France respectively. Note the presence of light brownish spots on all the dark brown flints.

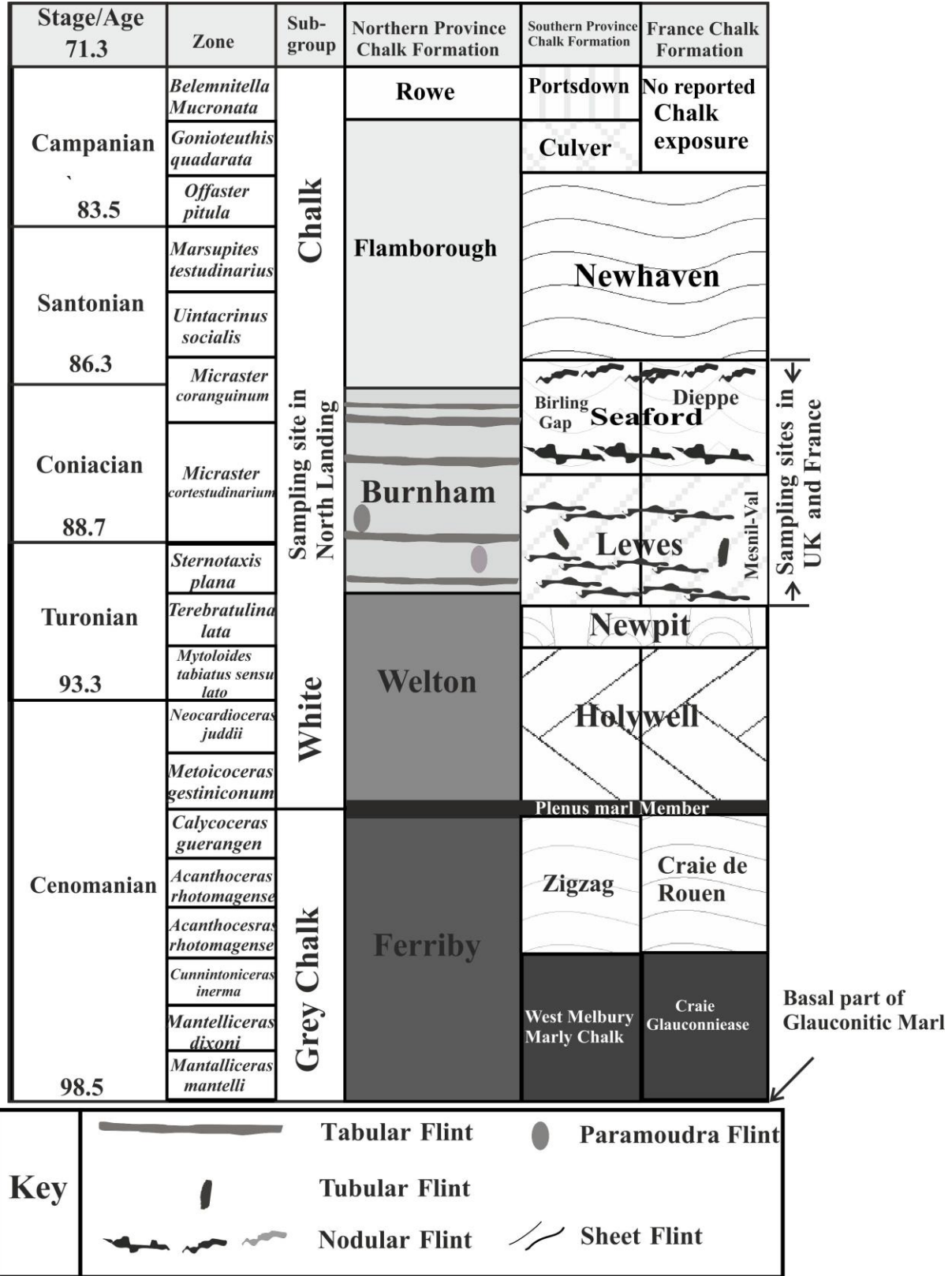


Fig. 4. Simplified Stratigraphy of the Upper Cretaceous Chalk in the study sites, contrasting the Northern Province chalks of northern east England with the Southern Province chalks of southern England and North France. The figure identifies and compares the main flint horizons in the chalk which were sampled, the key shows the main types of flint and where they occur in the stratigraphy (Adapted from Bristow et al., 1997; Mortimore et al. 2001; Mortimore 2011; Dupéret et al. 2012).

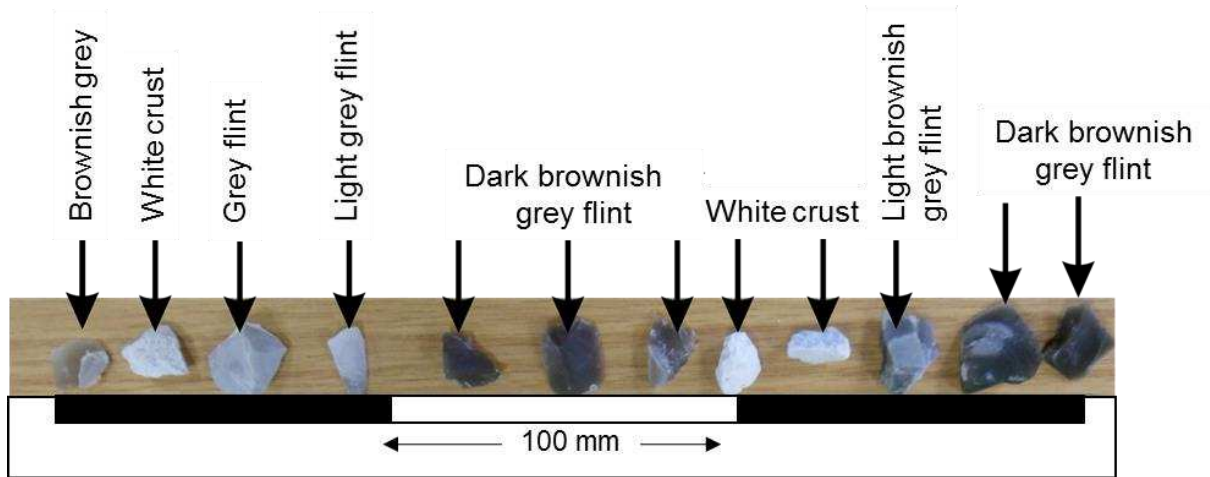
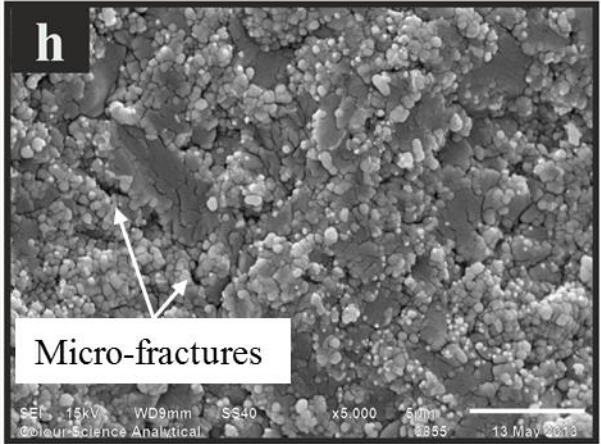
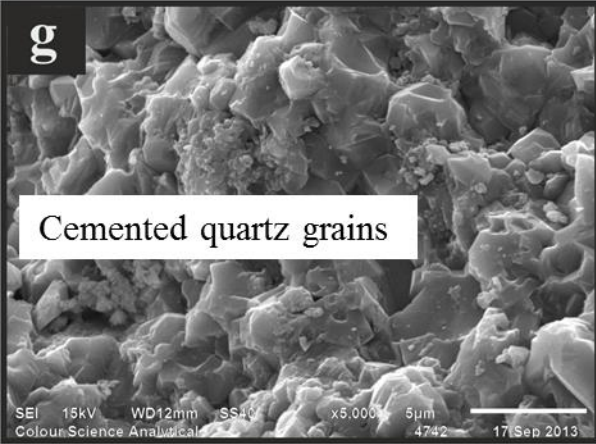
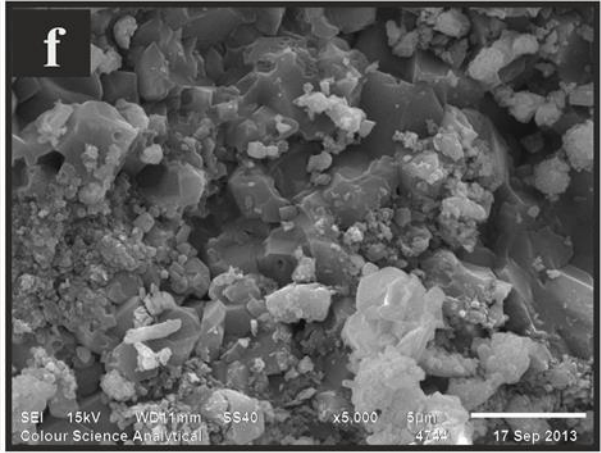
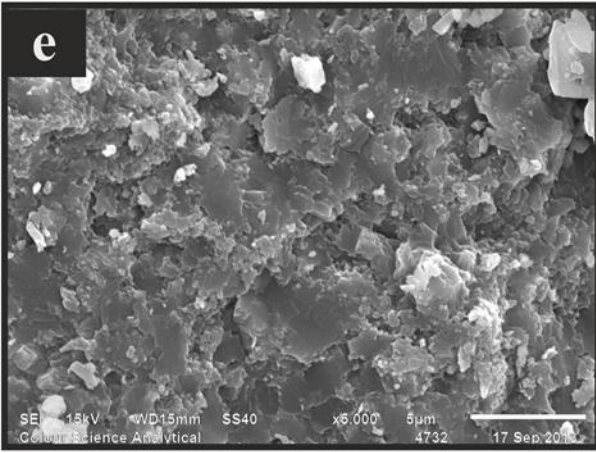
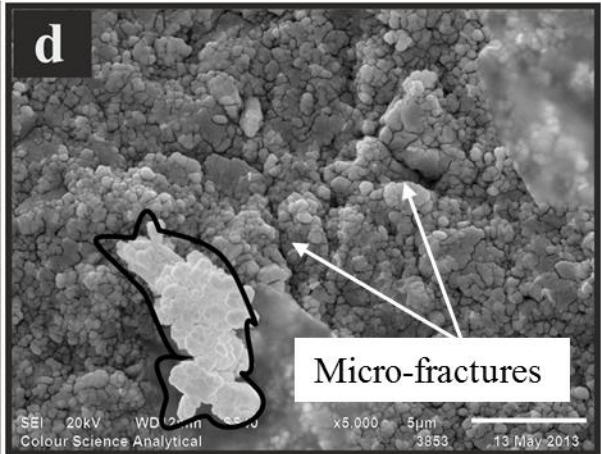
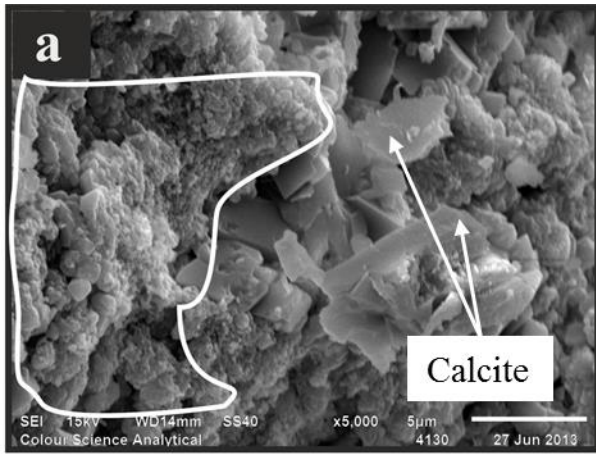


Fig. 5. Different flint structures and colours used for petrographic analysis.



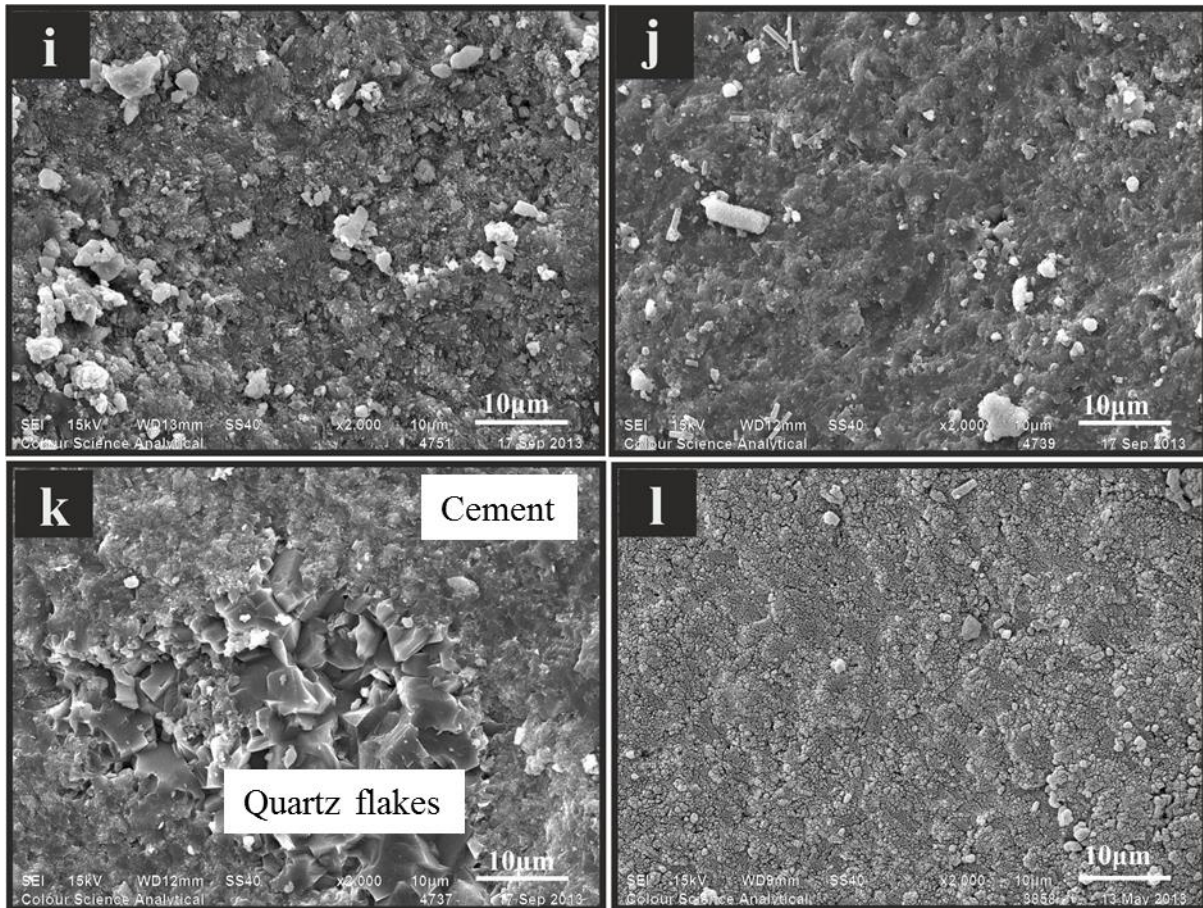


Fig. 6. SEM images flint samples showing different morphologies. (a) WCr from BNLUK with white arrows showing calcite crystals. White outline enclosed clusters of quartz crystals. (b) and (c) WCr SESUK, and WCr SDFr respectively with white outline enclosing amorphous silica particles with some silica cements (d) LBG from BNLUK matrix dominated spherical quartz grains with interparticle pores. Arrows show interparticle microfractures. Dark outline enclosed clusters of quartz crystals. (e) LBG from SESUK shows a matrix dominated by massive quartz cement. (f) LBG from SDFr shows a matrix rich in cemented quartz grains (g) LBG from LMFr showing a matrix dominated by cemented quartz grains. (h) BG from BNLUK showing microfractures, and equigranular microspheres forming clusters. The white arrows show interparticle microfractures. The matrix of this sample is dominated by quartz microspherules with some interparticle quartz cement. (i) DBG from SESUK shows a matrix dominated by massive quartz cement. (j) DBG from SDFr shows a matrix dominated by massive quartz cement. (k) DBG from LMFr shows a matrix dominated by massive quartz cement surrounding quartz flakes. (l) Grey Flint (GF) from BNLUK is a sample dominated by cemented spherical quartz grains.

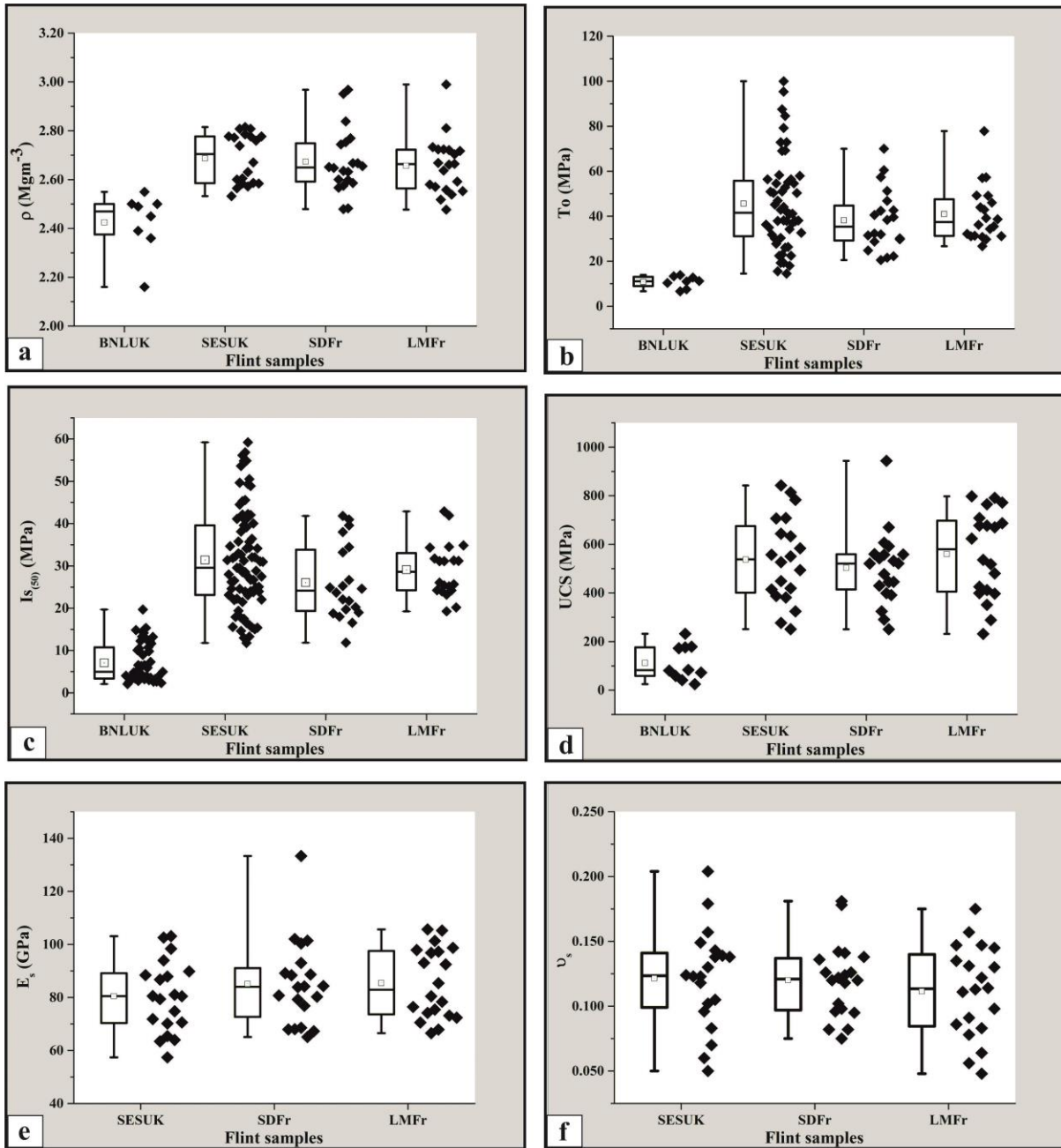


Fig. 7. (a) Density of flints (Mgm^{-3}); (b) Tensile strength (MPa); (c) Point load strength index (MPa); (d) UCS (MPa); (e) Static Young's Modulus (GPa); (f) Static Poisson's ratio of flints from all the study sites.

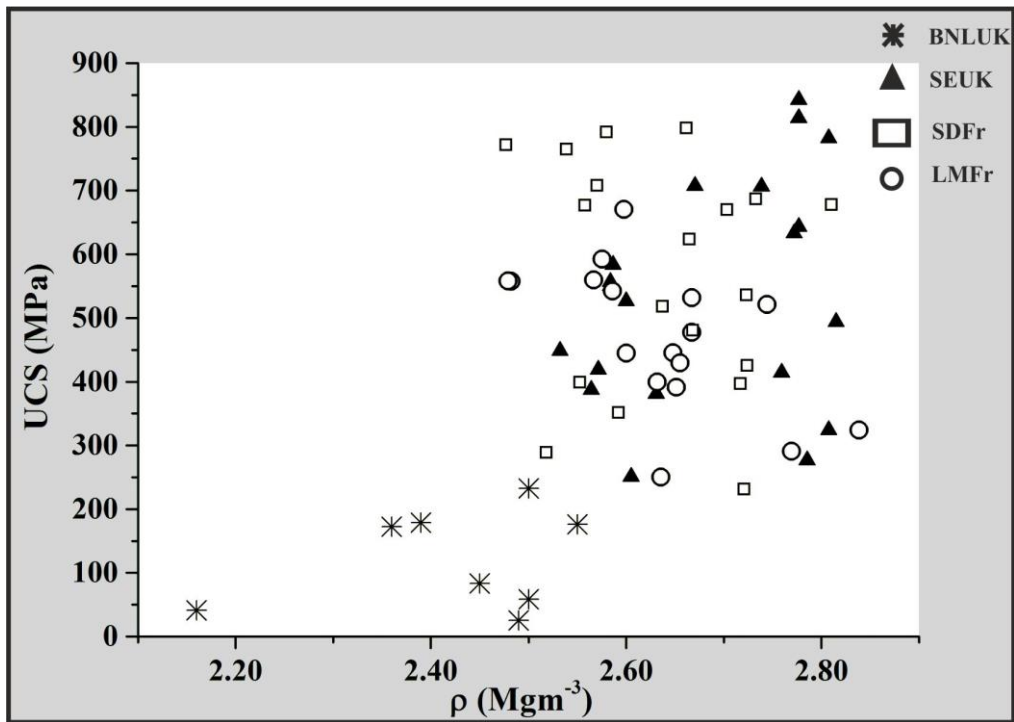


Fig. 8. UCS against density of flints

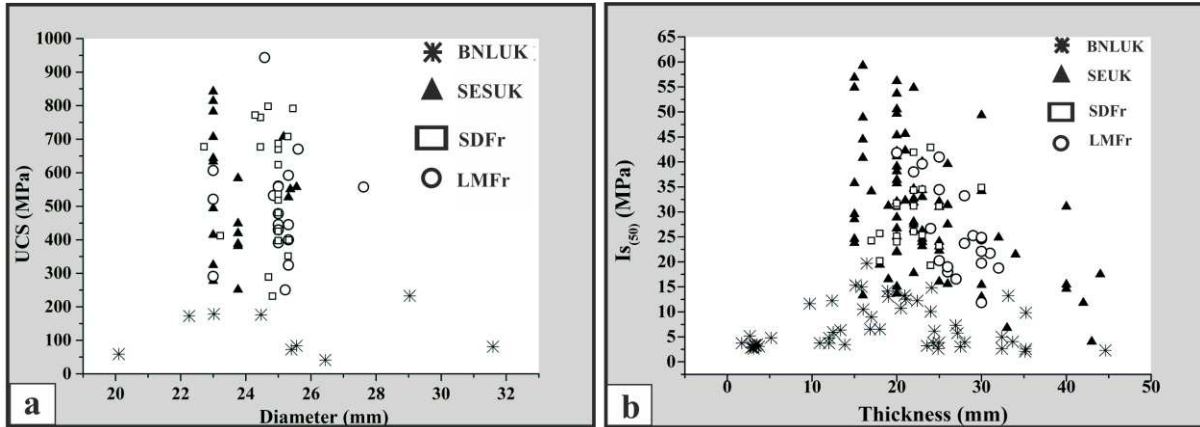


Fig 9. Sizes of samples against (a) UCS, (b) $I_{s(50)}$ of flints.

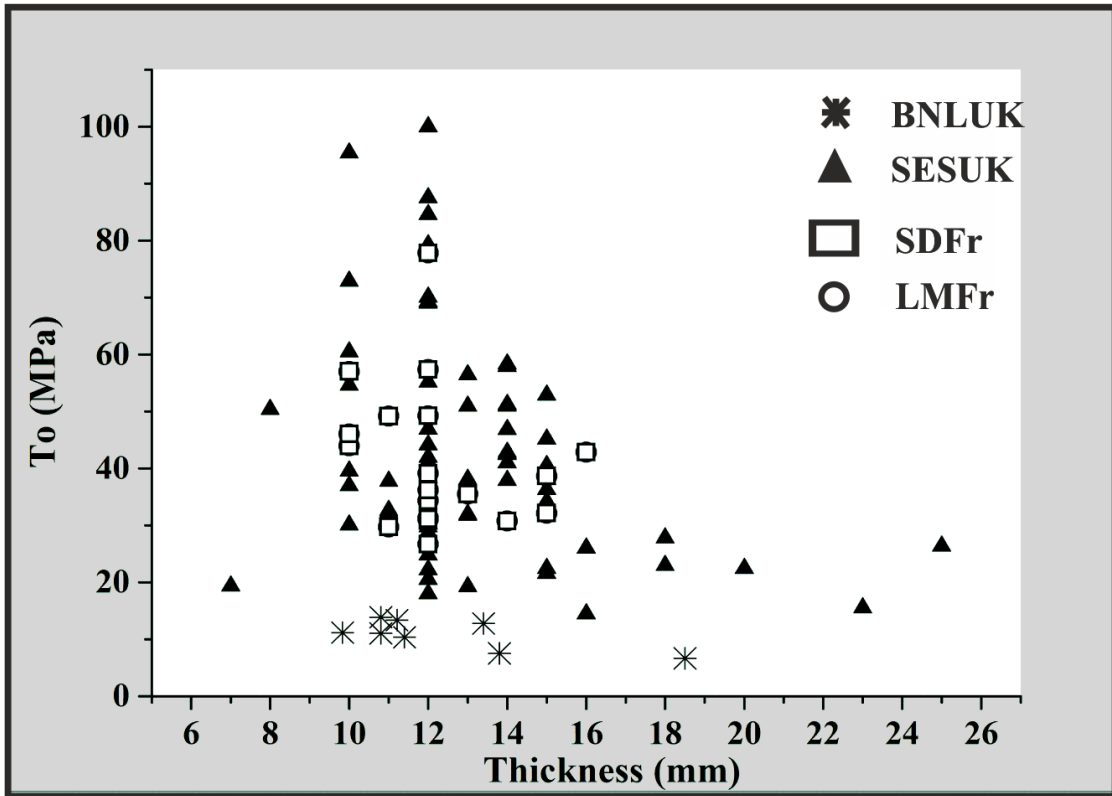


Fig. 10. Tensile strength of flint against sizes of flint samples.

Table 1. *Flint colour classification and Munsell colour chart code.*

Colour Description	Classification Code	Munsell Colour Code
White crust	WCr	-
Grey flint	GF	N5
Light brown flint	LBG	5YR 6/1
Brownish grey flint	BG	5G 2/1
Dark brown grey flint	DBG	5YR 2/1

Table 2. *Sampling sites, location and flint categories present.*

Location	Formation	Notation	Flint Type Present
North Landing, Yorkshire, UK	Burnham Chalk	Flint from Burnham Chalk North Landing, UK (BNLUK)	White crust (WCr)
			Light brown flint (LBG)
			Grey flint (GF)
East Sussex, UK	Seaford Chalk	Flint from Seaford Chalk, East Sussex, UK (SESUK)	White crust (WCr)
			Light brown flint (LBG)
			Brownish grey (BG)
Dieppe, France	Seaford Chalk	Flint from Seaford Chalk, Dieppe, France (SDFr)	Dark brown grey (DBG)
			White crust (WCr)
			Light brown flint (LBG)
Mesnil-Val Plage, France	Lewes Chalk	Flint from Lewes Chalk, Mesnil-Val, France (LMFr)	Brownish grey (BG)
			Light brown flint (LBG)
			Dark brown grey (DBG)

Note: The abbreviations used in this paper will follow the following format: FORMATION- LOCATION- COUNTRY. Therefore, a notation of BNLUK represents flint sample from the Burnham Chalk from North Landing in the UK. The exception to this notation is the white crusts (WCr).

Table 3. *Testing methods and specifications*

Property tested	Method	References
Density (ρ)	Caliper	ISRM (2007)
Tensile strength (T_o)	Three-Point Disc	Brook (1993)
Point Load Index ($I_{s(50)}$)	Block and irregular lump tests	Broch and Franklin (1972) ISRM 2007
Uniaxial Compressive strength (UCS) Test	Cylindrical and Cuboid shapes	ASTM D2845 2000
Young's Modulus	5mm electrical resistance strain gauges due to fine grain nature of the rock.	ASTM D7012-07 2010
Poisson's Ratio		ISRM 2007

Table 4. *Sample sizes and geometries used in the testing program*

Tests	Sample Sizes					Number of tests
	Length (mm)	Breadth (mm)	Depth (mm)	Diameter (mm)	L/D	
Three-Point Disc method	40-72	14-50	7-28	-	-	106
Point Load Strength	25-90	19-45	15-44	-	-	102
UCS (Cylinder)	48-77	-	-	23-37	2.1-2.5	60
UCS (Cuboidal)	50-68	23-32	18-29	-	2.0-3.5	12

Note: The UCS test was conducted in accordance with ASTM D2845 (2000); ASTM D7012-07 (2010) and ISRM (2007). Specimen specifications followed these standards. The specimen ends were prepared and flattened using surface grinder. Parallellism and flatness of the specimen ends were maintained within a tolerance of 0.02 mm, and within 0.30 mm for the straightness of specimen sides over the complete length of the specimen.

Table 5. Summary of normality test using Shapiro-Wilk

Flint Types		BNLUK	SEUK	SDFr	LMFr
Parameters	UCS (MPa)	N (11)	N (20)	N (20)	N (20)
	I _{s(50)} (MPa)	NN (49)	N (82)	N (20)	N (20)
	To (MPa)	N (8)	NN (55)	N (20)	NN (20)
	E _s (GPa)	-	N (20)	NN (20)	N (20)
	v _s	-	N (20)	N (20)	N (20)

Note: N refers to normally distributed, NN in bold refers to not normally distributed and numbers in bracket refers to the number of tests.

Table 6. Summary of mean, standard deviation and median (in bracket) of physical and mechanical properties of flints

Flints Class	UCS (MPa)	ρ (Mgm ³)	To (MPa)	I _{s(50)} (MPa)	E _s (GPa)	v _s
BNLUK	112.19±71.04 (81.01)	2.43±0.12 (2.47)	10.85±2.63 (11.11)	6.79±3.85 (4.97)	-	-
SESUK	537.23±176.41 (538.60)	2.69±0.10 (2.70)	43.01±20.61 (41.56)	29.01±6.89 (29.57)	80.49±13.34 (80.50)	0.122±0.035 (0.124)
SDFr	502.88±150.35 (520.99)	2.67±0.13 (2.65)	38.58± 13.65 (35.33)	26.06±8.93 (24.15)	85.13±16.12 (84.02)	0.120±0.121 (0.121)
LMFr	560.31±178.41 (579.76)	2.66±0.12 (2.66)	41.01±12.49 (37.43)	29.12±6.50 (28.59)	85.44±13.28 (82.91)	0.112±0.035 (0.114)

Table 7. 25th and 75th percentile of physical and mechanical properties of flints

Flint Class	Parameters	UCS (MPa)		ρ (Mgm ³)		To (MPa)		I _{s(50)} (MPa)		E _s (GPa)		v _s	
	Percentile (%)	25	75	25	75	25	75	25	75	25	75	25	75
	BNLUK	60.45	174.32	2.38	2.50	9.65	12.93	3.38	10.72	-	-	-	-
SESUK	407.78	674.90	2.59	2.78	31.43	55.47	23.48	39.34	70.47	88.76	0.101	0.141	
SDFr	422.25	559.03	2.59	2.75	29.49	43.68	19.54	33.52	74.75	91.05	0.098	0.137	
LMFr	408.52	692.06	2.57	2.72	31.26	46.83	24.25	32.37	73.90	97.40	0.085	0.138	

Table 8. *Mineral compositions of flints and white crust*

Classification	Location	Quartz (%)	Calcite (%)	Halite (%)
WCr	North Landing	35.64	64.36	-
	East Sussex	92.48	5.17	2.36
	Dieppe	98.51	1.12	0.38
LBG	North Landing	86.09	13.21	0.70
	East Sussex	98.02	1.98	-
	Dieppe	99.11	0.89	-
	Mesnil-Val	93.74	6.26	-
BG	North Landing	97.84	1.96	0.20
GF	North Landing	98.09	1.91	-
DBG	East Sussex	99.16	0.84	-
	Dieppe	99.50	0.50	-
	Mesnil-Val	98.79	1.21	-

Note: (-) Are samples whose strength properties cannot be determined due to size requirements of the testing methods.

Table 9. Mechanical and mineralogical data for flint comparing present paper with previous studies

Author/Source	Location/Flint types	ρ (Mgm ³)	UCS (MPa)	To (MPa)	I _{s50} (MPa)	E _s (GPa) v _s	Quartz (%) Calcite (%)
This paper	WCr	-	-	-	-	-	<u>35.64 - 98.51</u> 1.12 - 64.36
	DBG	2.66 - 2.69	502.88 - 560.31	38.58 - 43.01	26.06 - 29.12	<u>85.13 - 85.44</u> 0.112 - 0.122	<u>98.79 - 99.50</u> 0.50 - 1.21
	GF	2.43	112.19	10.85	6.79	80.49	<u>98.09</u> 1.91
	LBG	-	-	-	-	-	<u>86.09 - 99.11</u> 0.89 - 13.21
	Jakobsen et al. 2014	Flint from Tyra Field, North Sea	-	-	-	-	-
Garcek 2007	α - Quartz	-	-	-	-	0.079	-
Smith et al. 2003	Brighton & Cray, UK	-	419	-	14.94	-	-
Pabst & Gregorová 2013	Low Quartz	-	-	-	-	<u>95.40</u> 0.082	-
Cumming 1999	Southern Province, UK	-	777	49.54	24.32	-	-
Fowell & Martin 1997 (Report)	Portsmouth	-	832	34.30	-	-	-
Cumming & Kageson-Loe 1995 (Report)	Bermondsey, London	-	-	-	7.60	-	-
Varley 1990	Killinghome	-	332	-	-	-	-
Waite 1985	Cromer	-	414	-	-	-	-
Pradel et al. 1967 & 1972	Grey Illustrious	-	409	57.00	-	-	-
	Grand Pressigny	-	391	68.00	-	-	-
	Fontmaure Jasper	-	57 - 178	8.00 - 38.00	-	-	-
	Grey Non lustrous	-	244	-	-	-	-
	English Flint	-	-	59.00 - 93.00	-	-	-
Iller 1963	Chalcedony	-	-	81.00 - 82.00	-	-	-
	Fused Silica	-	-	35.00 - 63.00	-	-	-
Weymouth & Williamson 1951	Flint	2.62	-	-	-	-	-
Washburn & Navias 1922	Flint	2.65	-	-	-	-	-

